

Electromagnetic Observables in Few-Nucleon Systems

Sonia Bacca

Received: date / Accepted: date

Abstract The electromagnetic probe is a very valuable tool to study the dynamics of few nucleons. It can be very helpful in shedding light on the not yet fully understood three-nucleon forces. We present an update on the theoretical studies of electromagnetic induced reactions, such as photo-disintegration and electron scattering off ^4He . We will show that they potentially represent a tool to discriminate among three-nucleon forces. Then, we will discuss the charge radius and the nuclear electric polarizability of the ^6He halo nucleus.

Keywords Electromagnetic probe · Reactions · Halo nuclei

1 Introduction

The interactions among nucleons are governed by quantum chromodynamics (QCD). In the low energy regime relevant to nuclear physics, QCD is not perturbative and thus difficult to solve. A series of models have been devised in the literature to describe nuclear forces in terms of effective degrees of freedom, protons and neutrons. Different approaches have been investigated, from pure phenomenology to theories based on meson exchanges and more recently to the systematic approach of effective field theory [1, 2]. For the nucleon-nucleon (NN) sector, several potentials are available that fit NN scattering data with high accuracy. On the other hand, since the nuclear potential has an effective nature, it is in principle a many-body operator. So one expects three-body forces ($3NF$) to be important. Hence, a debate is taking place regarding the role of $3NF$ s and how they can be constrained.

Presented at the 20th International IUPAP Conference on Few-Body Problems in Physics, 20 - 25 August, 2012, Fukuoka, Japan

S. Bacca
TRIUMF
4004 Wesbrook Mall
Vancouver, BC V6T 2A3, Canada
Tel.: +1 604-222-7372
Fax: +1 604-222-1074
E-mail: bacca@triumf.ca

For the determination of realistic three-body potentials or to discriminate among different models, one needs to find some few-nucleon observables involving at least three nucleons that show sensitivity to the different nuclear Hamiltonians. One also needs to perform these studies in the framework of few-body systems, where one can use exact calculations to test the nuclear interactions from a comparison to experiment. An important activity in this direction has taken place in recent years, with calculations of bound-state and hadronic scattering properties of light nuclei. Electromagnetic observables are complementary quantities that need to be investigated as well to shed more light on the not yet fully understood three-nucleon forces. In this paper we will present an update on recent studies of electromagnetic observables and we will limit the discussion to the well bound ${}^4\text{He}$ nucleus and to ${}^6\text{He}$ as an example in halo nuclei.

The paper is structured in the following way. In Sec. 2 we will first present the main calculational techniques: most of the results shown here have been obtained using the hyper-spherical harmonics method and the Lorentz integral transform for break-up reactions. In Sec. 3 we will talk about ${}^4\text{He}$ and in Sec. 4 about ${}^6\text{He}$. Finally, in Sec. 5 we will draw some conclusions.

2 Theoretical tools

For a given Hamiltonian H one can use the hyper-spherical harmonics (HH) expansion to solve the Schrödinger equation $H|\Psi\rangle = E|\Psi\rangle$. This method is typically employed in few-body systems with 3 or 4 constituents, but it can be successfully applied to 6-body calculations as well [3]. The approach is translationally invariant, being constructed starting from the Jacobi coordinates. It is also very accurate for bound states. In the HH method, the wave-function expansion reads

$$|\Psi\rangle = \sum_{[K]n}^{K_{\max}, n_{\max}} C_{[K]n} R_n(\rho) \mathcal{Y}_{[K]}(\Omega, s_1, \dots, s_A, t_1, \dots, t_A), \quad (1)$$

where $\mathcal{Y}_{[K]}$ are the HH and $R_n(\rho)$ are the hyper-radial wave functions, which are expressed in terms of Laguerre polynomials. Here, s_i and t_i are the spin and isospin of nucleon i , respectively. $C_{[K]n}$ is the coefficient of the expansion labeled by a cumulative quantum number $[K]$, which includes the grand-angular momentum K , and by n for the hyper-radial states.

We are not only interested in bound state properties, but in electromagnetic induced reactions as well. In this case, a fundamental ingredient is the inclusive nuclear response function

$$R_O(\omega, q) = \sum_f |\langle \Psi_f | O(q) | \Psi_0 \rangle|^2 \delta(E_f - E_0 - \omega), \quad (2)$$

where ω and q are the energy and momentum transferred, $|\Psi_{0/f}\rangle$ and $E_{0/f}$ denote initial and final state wave functions and energies. Finally O represents a general excitation operator. From Eq. (2) it is evident that in principle one needs the knowledge of all possible final states in the continuum. This fact constitutes a

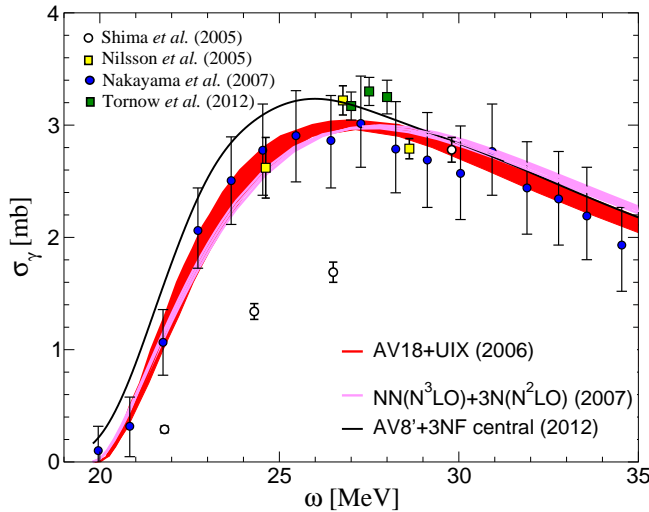


Fig. 1 (Color online) Total ${}^4\text{He}$ photo-absorption cross section: calculations with the AV18+UIX from [5], with EFT forces from [7] and with a central $3NF$ from [8] in comparison with data obtained with tagged photons (see Ref. [5] for all experimental reference).

major complication, which we circumvent by using the Lorentz integral transform (LIT) method [4]. This reduces the problem to the solution of the equation

$$(H - E_0 - \sigma)|\tilde{\Psi}_{\sigma,q}^O\rangle = O(q)|\Psi_0\rangle, \quad (3)$$

where σ is a complex parameter and $|\tilde{\Psi}_{\sigma,q}^O\rangle$ is a state with bound-state-like asymptotics. Eq.(3) is then solved with the HH expansion.

3 The stable ${}^4\text{He}$ nucleus

In the following we will present results for electromagnetic induced reactions for the nucleus of ${}^4\text{He}$.

Photo-disintegration cross section. We start our discussion from the photo-disintegration cross section of ${}^4\text{He}$. Such nucleus is the ideal testing ground for microscopic three-body forces, which are often fitted in three-body bound systems. Furthermore, because of gauge invariance, nuclear forces also manifest themselves as exchange currents in photo-reactions. In the last three decades there has been a continuous interest in the photo-disintegration of ${}^4\text{He}$. The latest results, both from theory and experiment, are of 2012. The total cross section σ_γ can be calculated as

$$\sigma_\gamma(\omega) = 4\pi^2\alpha\omega R_{E1}(\omega), \quad (4)$$

where α is the fine structure constant and $R^{E1}(\omega)$ is a response function as in Eq.(2), with $q = \omega$. The operator is the electric dipole operator $O = E1$. The dominant part of the exchange currents contribution is taken into account in the dipole response function via the Siegert theorem. In Ref. [5] we calculated σ_γ

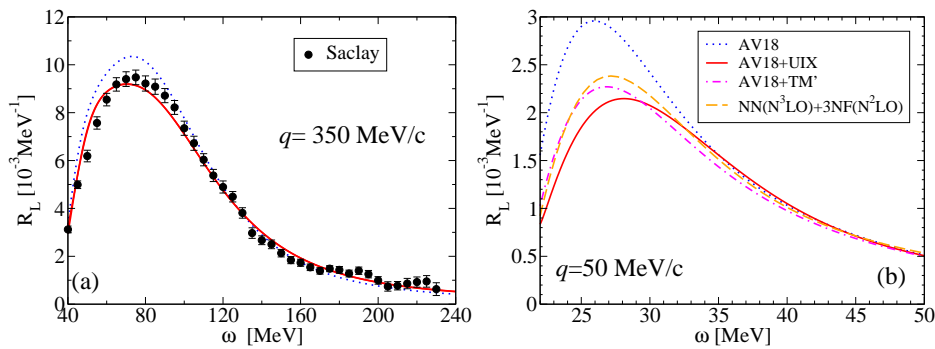


Fig. 2 (Color online) Panel (a): $R_L(\omega)$ at $q = 350$ MeV/c with the AV18 (dotted), AV18+UIX (solid) potentials in comparison with the experimental data from Saclay. Panel (b): $R_L(\omega)$ at $q = 50$ MeV/c with the same potentials, with the AV18+TM' force (dash-dotted) and a preliminary results from chiral forces (dashed) with NN at N^3LO and $3NF$ at N^2LO .

for the first time using the realistic potential AV18+UIX [6]. One year later, σ_γ was calculated from chiral EFT potentials using the LIT method in conjunction with the no core shell model [7], leading to a very similar result. In 2012 a new calculation was performed with the complex scaling method [8] using a very simple purely central three-body force. All these theoretical curves are shown in Fig. 1. Except from threshold, where [8] is not accurate, the H -dependence of the cross section at the peak is of the order of 10%. This is much less than the difference in the experimental data. In particular, the data from Shima *et al.* [9] are a factor of 2 smaller than all other measurements including the latest experiment from 2012 [10]. Because the theoretical sensitivity to changes in the Hamiltonians is smaller than the difference in the experiments, it is unfortunately not yet possible to discriminate among $3NF$ s.

Electron scattering reaction. In the one-photon-exchange approximation, the inclusive cross section for electron scattering off a nucleus is given in terms of two response functions, i.e.

$$\frac{d^2\sigma}{d\Omega d\omega} = \sigma_M \left[\frac{Q^4}{q^4} R_L(\omega, q) + \left(\frac{Q^2}{2q^2} + \tan^2 \frac{\theta}{2} \right) R_T(\omega, q) \right] \quad (5)$$

where σ_M denotes the Mott cross section; $Q^2 = -q_\mu^2 = q^2 - \omega^2$ is the squared four momentum transfer with q being the three-momentum transfer; θ is the electron scattering angle. $R_L(\omega, q)$ and $R_T(\omega, q)$ are the longitudinal and transverse response functions, respectively. In the following we will discuss R_L , which is a function like that in Eq. (2) with $O = \rho(q)$, where $\rho(q)$ is the Fourier transform of the charge density operator. R_L is well known for not being very sensitive to exchange currents, so one can concentrate in studying the sensitivity of this observable to $3NF$. In Refs. [11,12] we performed for the first time a calculation of R_L at different q values with different realistic potentials. We found that the experimental results are better described by theory if one includes $3NF$, as one can see from Fig. 2(a). We also performed calculations at low momentum transfer, where no experimental data have been published yet. We observed that the difference between calculations with NN only and calculations which include $3NF$ s

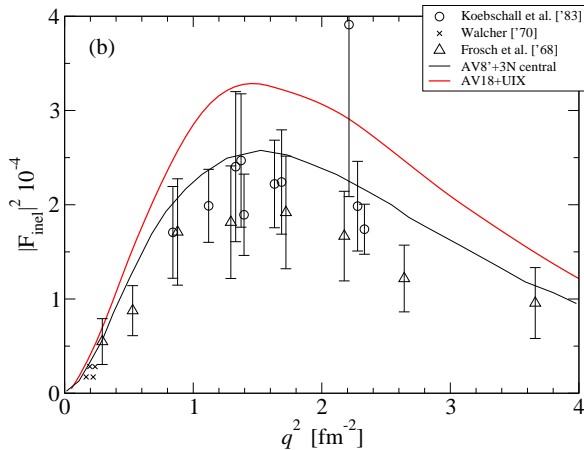


Fig. 3 (Color online) Inelastic form factor to the first 0^+ excited state of ${}^4\text{He}$: calculation with a central $3NF$ by Hiyama *et al.* [13] and with the AV18+UIX force (*preliminary*) in comparison to the available experimental data.

is increasing at low q , reaching even 50% at $q = 50$ MeV/c. In Fig. 2(b) we also show the sensitivity to different three-body Hamiltonians. It is such, that precise data can potentially discriminate among realistic potentials.

Recently, we have studied the inelastic transition form factor $F_{\text{inel}}(q)$ to the first excited state 0^+ of ${}^4\text{He}$. This quantity can be also measured from electron scattering experiments and several data sets are available. Theoretically, $F_{\text{inel}}(q)$ is an inelastic observable with transitions into the continuum which are induced only by the $\ell = 0$ component of R_L . The first calculation was performed by Hiyama *et al.* [13] with a simple purely central $3NF$ and using bound state techniques. A good description of data was achieved. We performed a calculation of $F_{\text{inel}}(q)$ treating the continuum problem with the Lorentz integral transform method and using more sophisticated $3NFs$. Our *preliminary* results are shown in Fig. 3 (see other FB20 proceedings [14] for more details). These findings point toward a large sensitivity of $F_{\text{inel}}(q)$ to the nuclear Hamiltonian, which can be potentially used to discriminate among different $3NFs$ if precise data become available.

4 The unstable ${}^6\text{He}$ nucleus

In the following we will discuss the charge radius and the nuclear electric polarizability of ${}^6\text{He}$.

The nuclear charge radius. ${}^6\text{He}$ is a radioactive halo nucleus that undergoes β -decay with a half-life of 0.8 s. Because ${}^6\text{He}$ is a relatively light nucleus, one can perform *ab-initio* calculations and test nuclear forces from a comparison with experiment. Electron scattering cannot be easily performed on unstable nuclei, so to learn about the proton distribution, a viable way is to use laser spectroscopy techniques. The charge radius r_{ch} of ${}^6\text{He}$ was measured in [15] and has been recently reevaluated using input from the first direct mass measurement [16], leading to $r_{\text{ch}} = 2.060 \pm 0.008$ fm. This can be converted into a point-proton radius, which is what *ab-initio*

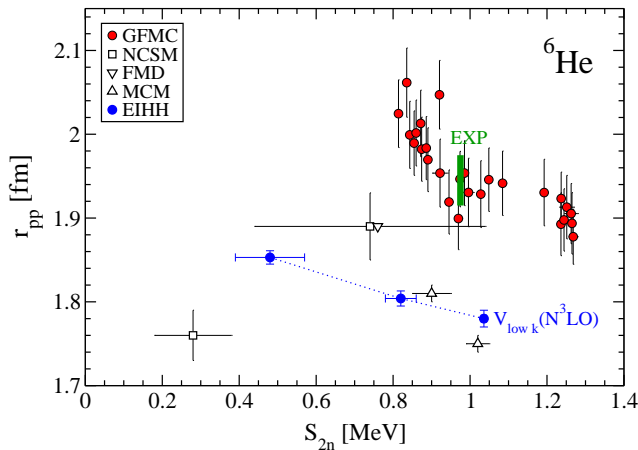


Fig. 4 (Color online) Correlation plot of the ${}^6\text{He}$ point-proton radius versus two-neutron separation energy S_{2n} . The experimental range, shown by the bar, is compared to theory based on different methods (NCSM [20], FMD [21], MCM [22]) and to our results with $V_{\text{low } k}$. Only the GFMC [19] calculations include $3NF$.

theories can calculate. We recently have performed a chiral EFT based study of ${}^6\text{He}$ [17], limited to two-body forces, where low-momentum interactions $V_{\text{low } k}$ [18] were employed in conjunction with HH expansions of the wave function. Here, we present a combined comparison of our results to experiment and other *ab-initio* calculations (GFMC from [19], NCSM from [20], FMD from [21] and MCM from [22]) by showing a plot of the point-proton r_{pp} radius versus the two-neutron separation energy S_{2n} in Fig. 4. The cutoff Λ dependence of our results with $V_{\text{low } k}$ allows us to study the correlation between these observables: the radius increases as the separation energy decreases, as one expects. Our calculations do not reproduce simultaneously r_{pp} and S_{2n} : there exists an optimal value of Λ where S_{2n} is predicted in accordance with experiment, but r_{pp} is not reproduced and vice-versa. Also, we would like to note that all other calculations omit $3NF$, except from the GFMC points [19], which are the only ones going through the experimental band. This points towards the dependence of the charge radius upon H and towards the importance of including three nucleon forces.

The nuclear electric polarizability The nuclear electric polarizability α_E is related to the response of the nucleus to an externally applied electric field and is relevant in the extraction of nuclear quantities from atomic spectroscopic measurements. The atomic energy levels, in fact, are affected by polarization of the nucleus due to the electric field of the surrounding electrons. The polarizability of a soft halo nucleus is measured to be a lot bigger than that of ${}^4\text{He}$. Thus, it is interesting to study if this is reproduced by theory and whether the experimental data is explained. The nuclear electric polarizability in the dipole approximation is defined by

$$\alpha_E = 2\alpha \sum_{f \neq 0} \frac{|\langle \Psi_f | E1 | \Psi_0 \rangle|^2}{E_f - E_0}. \quad (6)$$

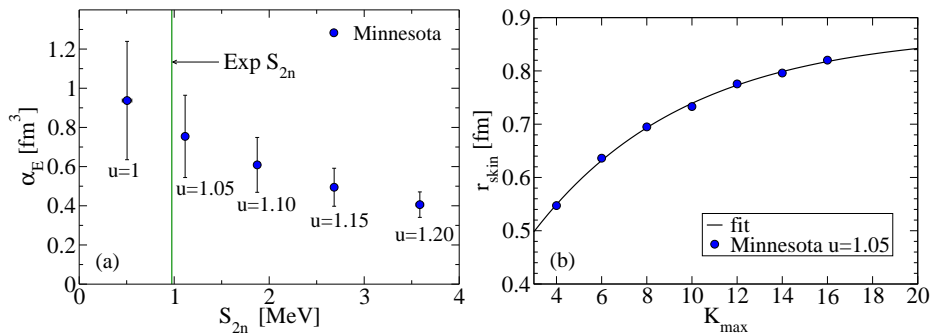


Fig. 5 (Color online) Panel (a): Correlation between α_E and S_{2n} in ${}^6\text{He}$ obtained with the Minnesota potential varying the parameter u . The model space used here is $K_{\text{max}} = 12/13$. Panel (b): Neutron skin radius r_{skin} of ${}^6\text{He}$ with the Minnesota potential and $u = 1.05$, as a function of the grand-angular momentum quantum number K_{max} . The curve is a fit to the calculated points, used to extrapolate to infinite model space.

It is clearly related to the photo-absorption cross section by

$$\alpha_E = \frac{m_{-2}(\infty)}{2\pi^2} \text{ with } m_n(\bar{\omega}) \equiv \int_{\omega_{th}}^{\bar{\omega}} d\omega \omega^n \sigma_\gamma(\omega), \quad (7)$$

where σ_γ can be calculated exactly with the Lorentz Integral transform method. We recently have performed such calculation for ${}^6\text{He}$ [23], using a simple semi-realistic potential, the Minnesota force, which reproduces the experimental value of the polarizability of ${}^4\text{He}$ reasonably well. Within this force model one can add attractive P -wave interactions by changing the parameter u (see [23] for details). This mostly affects the binding of ${}^6\text{He}$, without substantially changing ${}^4\text{He}$. By varying u we first observed a correlation of α_E vs S_{2n} , as shown in Fig. 5(a). We have chosen u so that the halo feature, represented by S_{2n} , is reproduced. We have then studied the correlations between other two observables: α_E and the skin radius r_{skin} . The latter is defined as $r_{\text{skin}} = r_n - r_p$, where r_n and r_p are the mean point-neutron and point-proton radii. By varying the HH model space we observed that α_E and r_{skin} are correlated linearly as $\alpha_E = a + b r_{\text{skin}}$. From our theoretical data we have “measured” the coefficients a and b and then we used them to estimate the polarizability out of a bound-state calculation. The calculation of r_{skin} , in fact, does not require an expansion on the dipole excited states and as such is less computationally demanding and can be performed for larger model spaces ($K_{\text{max}} = 16$). The convergence of r_{skin} is shown in Fig. 5(b). Extrapolating the points with an exponential *ansatz* of the form $r_{\text{skin}}(K_{\text{max}}) = r_{\text{skin}}(\infty) - ce^{-\kappa K_{\text{max}}}$ we get $r_{\text{skin}}(\infty) = 0.87(5)$ fm. Using this skin radius and the linear dependence, we estimate the theoretical nuclear electric polarizability of ${}^6\text{He}$ to be $\alpha_E = 1.00(13)$ fm³. Even though theory correctly predicts $\alpha_E({}^6\text{He})$ to be one order of magnitude larger than the $\alpha_E({}^4\text{He})$, $\alpha_E({}^6\text{He})$ is about a factor of two smaller than the experimental value [24] of $\alpha_E^{\text{exp}} = 1.99(40)$ fm³. This points toward a potential disagreement of theory with experiment. The sensitivity of α_E with respect to different H , that reproduce S_{2n} will be investigated in the future.

5 Conclusions

In conclusion, because electromagnetic observables show sensitivity to the nuclear Hamiltonians, they need to be further investigated both in theory and experiment. They have the potential of shedding more light on the not yet fully understood three-nucleon forces.

Acknowledgements It is a pleasure to thank the organizers for the very interesting conference and for providing a stimulating environment. I would like to thank my collaborators Nir Barnea, Raymond Goerke, Winfried Leidemann, Giuseppina Orlandini and Achim Schwenk, whose help has been fundamental in obtaining the results shown in this proceedings. This work was supported by the Natural Sciences and Engineering Research Council (NSERC) and by the National Research Council of Canada.

References

1. Entem, D.R., and Machleidt, R.: Chiral effective field theory and nuclear forces. *Phys. Rept.* 503, 1 (2011)
2. Epelbaum, E., Hammer, H.-W., U.-G. Meißner, U.-G.: Modern Theory of Nuclear Forces. *Rev. Mod. Phys.* 81, 1773 (2009)
3. Barnea, N., Leidemann, W., Orlandini, G.: State dependent effective interaction for the hyperspherical formalism. *Phys. Rev. C* 61, 054001 (2000)
4. Efros, V.D., Leidemann, W., Orlandini, G.: Response functions from integral transforms with a Lorentz kernel. *Phys. Lett. B* 338, 130 (1994)
5. Gazit, D., Bacca, S., Barnea, N., Leidemann, W., Orlandini, G.: Photoabsorption on ^4He with a Realistic Nuclear Force. *Phys. Rev. Lett.* 96, 112301 (2006)
6. Wiringa, R.B., Stoks, V.G.J., Schiavilla, R.: Accurate nucleon-nucleon potential with charge-independence breaking. *Phys. Rev. C* 51, 38 (1995)
7. Quaglioni, S. and Navratil, P.: The ^4He total photo-absorption cross section with two- plus three-nucleon interactions from chiral effective field theory. *Phys. Lett. B* 652 (2007) 370
8. Horiuchi, W., Suzuki, Y., Arai, K.: Ab initio study of the photoabsorption of ^4He . *Phys. Rev. C* 85, 054002 (2012)
9. Shima, T. *et al.*: Simultaneous measurement of the photodisintegration of ^4He in the giant dipole resonance region. *Phys. Rev. C* 72, 044004 (2005)
10. Tornow, W. *et al.*: Photodisintegration cross section of the reaction $^4\text{He}(\gamma, n)^3\text{He}$ at the giant dipole resonance peak, *Phys. Rev. C* 85, 061001 (2012); Raut, R. *et al.*: Photodisintegration Cross Section of the Reaction $^4\text{He}(\gamma, p)^3\text{H}$ between 22 and 30 MeV. *Phys. Rev. Lett.* 108, 042502 (2012)
11. Bacca, S., Barnea, N., Leidemann, W., Orlandini, G.: Role of final state interaction and of three-body force on the longitudinal response function of ^4He . *Phys. Rev. Lett.* 102, 162501 (2009)
12. Bacca, S., Barnea, N., Leidemann, W., Orlandini, G.: Search for three-body force effects on the longitudinal response function of ^4He . *Phys. Rev. C* 80, 064001 (2009)
13. Hiyama, E., Gibson, B.F., and Kamimura, M.: Four-body calculation of the first excited state of ^4He using a realistic NN interaction: $^4\text{He}(e, e)^4\text{He}(0_2^+)$ and the monopole sum rule. *Phys. Rev. C* 70, 031001 (2004)
14. Orlandini, G., Bacca, S., Barnea, N., Leidemann, W.: The Isoscalar Monopole Resonance of ^4He . Proceedings of the FB20 conference.
15. Wang, L.B. *et al.*: Laser Spectroscopic Determination of the ^6He Nuclear Charge Radius: *Phys. Rev. Lett.* 93, 142501 (2004)
16. Brodeur, M., Brunner, T., Champagne, C., Effenauer, S., Smith, M.J., Lapierre, A., Ringle, R., Ryjckov, V.L., Bacca, S., Delheij, P., Drake, G.W.F., Lunney, D., Schwenk, A., Dilling, J.: First direct mass-measurement of the two-neutron halo nucleus ^6He and improved mass for the four-neutron halo ^8He . *Phys. Rev. Lett.* 108, 052504 (2012)
17. Bacca, S., Barnea, N., Schwenk, A.: Matter and charge radius of ^6He in the hyperspherical-harmonics approach. *Phys. Rev. C* 86, 034321 (2012)

18. Bogner, S.K., Furnstahl, R.J., Schwenk, A.: From low-momentum interactions to nuclear structure. *Prog. Part. Nucl. Phys.* 65, 94 (2010)
19. Pieper, S.C.: Quantum Monte Carlo Calculations of Light Nuclei. *Riv. Nuovo Cim.* 31, 709 (2008)
20. Caurier, E. and Navratil, P.: Proton radii of ${}^4,6,8\text{He}$ isotopes from high-precision nucleon-nucleon interactions: *Phys. Rev. C* 73, 021302(R) (2006)
21. Neff, T., Feldmeier, H.: Cluster structures within Fermionic Molecular Dynamics. *Nucl. Phys. A* 738, 357 (2004)
22. Brida, I., Nunes, F.N.: Two-neutron overlap functions for ${}^6\text{He}$ from a microscopic structure model. *Nucl. Phys. A* 847, 1 (2010)
23. Goerke, R., Bacca, S., Barnea, N.: The nuclear electric polarizability of ${}^6\text{He}$. [arXiv:1209.2468](https://arxiv.org/abs/1209.2468)
24. Pachucki, K., Moro, A.M.: Nuclear polarizability of helium isotopes in atomic transitions. *Phys. Rev. A* 75, 032521 (2007)